Transcriptional Activation by CprK1 Is Regulated by Protein Structural Changes Induced by Effector Binding and Redox State*[S]

Hortense Mazon[‡], **Krisztina Gábor**[§], **David Leys**[¶], **Albert J. R. Heck**[‡], **John van der Oost**[§], **and Robert H. H. van den Heuvel**[‡1]

From the [‡]*Department of Biomolecular Mass Spectrometry, Bijvoet Center for Biomolecular Research and Utrecht Institute for Pharmaceutical Sciences, Utrecht University, Sorbonnelaan 16, 3584 CA Utrecht, The Netherlands, the* [§]*Laboratory of Microbiology, Wageningen University and Research Centre, Hesselink van Suchtelenweg 4, 6703 CT Wageningen, The Netherlands, and the* [¶]*Faculty of Life Sciences, Manchester Interdisciplinary Biocentre, University of Manchester, Manchester M60 1QD, United Kingdom*

The transcriptional activator CprK1 from *Desulfitobacterium hafniense*, a member of the ubiquitous cAMP receptor protein/fumarate nitrate reduction regulatory protein family, activates transcription of genes encoding proteins involved in reductive dehalogenation of chlorinated aromatic compounds. 3-Chloro-4-hydroxyphenylacetate is a known effector for CprK1, which interacts tightly with the protein, and induces binding to a specific DNA sequence ("dehalobox," TTAAT—-ATTAA) located in the promoter region of chlorophenol reductive dehalogenase genes. Despite the availability of recent x-ray structures of two CprK proteins in distinct states, the mechanism by which CprK1 activates transcription is poorly understood. In the present study, we have investigated the mechanism of CprK1 activation and its effector specificity. By using macromolecular native mass spectrometry and DNA binding assays, analogues of 3-chloro-4-hydroxyphenylacetate that have a halogenated group at the *ortho* position and a chloride or acetic acid group at the *para* position were found to be potent effectors for CprK1. By using limited proteolysis it was demonstrated that CprK1 requires a cascade of structural events to interact with dehalobox dsDNA. Upon reduction of the intermolecular disulfide bridge in oxidized CprK1, the protein becomes more dynamic, but this alone is not sufficient for DNA binding. Activation of CprK1 is a typical example of allosteric regulation; the binding of a potent effector molecule to reduced CprK1 induces local changes in the N-terminal effector binding domain, which subsequently may lead to changes in the hinge region and as such to structural changes in the DNA binding domain that are required for specific DNA binding.

Halogenated hydrocarbons are often toxic molecules. They are widespread environmental pollutants because of their numerous applications, for example in industry (degreasers), agriculture (pesticides), and private households (flame retardants). Although these compounds are generally very stable, they can be converted in many sediments and soils by reductive dehalogenation. Several strictly anaerobic bacteria capable of dehalogenation have been isolated including *Desulfomonile*, *Dehalobacter*, and *Desulfitobacterium*. These organisms use chlorinated compounds as terminal electron acceptors (halorespiration) and thus remove the chloride atom while energy is conserved via electron transport phosphorylation (1–3). The prospect of using these organisms in bioremediation of sediments contaminated with a variety of chlorinated aromatic compounds is promising. *Desulfitobacterium dehalogenans* can reductively dechlorinate phenolic compounds at the *ortho* position (4, 5), and the closely related *Desulfitobacterium hafniense* DCB-2 (6) can dechlorinate phenolic compounds at the *ortho* and *meta* position; the latter reaction, however, is described only for 3,5-dichlorophenol (3,5-DCP)[2] as a substrate (7).

A large number of the proteins involved in halorespiration are encoded in the chlorophenol reductive dehalogenase (*cpr*) gene cluster, which contains *cprTK$_1$ZEBA$_1$C* open reading frames in *D. hafniense*. The product of the *cprA1* gene, a 3-chloro-4-hydroxyphenylacetate (CHPA) reductive dehalogenase has been isolated and characterized from *D. hafniense* (8). It was found that the *cprA1* gene is induced by the electron acceptor CHPA. The activation by CHPA is carried out at the transcription level by CprK1, a transcriptional activator protein that is encoded in the same *cpr* gene cluster. CprK1 is a member of the CRP/FNR (cAMP receptor protein/fumarate nitrate reduction regulatory protein) family of regulators that is ubiquitous in bacteria (9). CrpK1 from *D. hafniense* binds to a specific DNA sequence ("dehalobox," TTAAT—-ATTAA), located in the promoter region of several *cpr* genes including *cprA1*, with high affinity in the presence of CHPA. This enables

---

[S] The on-line version of this article (available at http://www.jbc.org) contains supplemental Tables S1 and S2 and Figs. S1–S6.

[1] To whom correspondence should be addressed: Organon, P.O. Box 20, 5340 BH Oss, The Netherlands. Tel.: 31-30-2536797; Fax: 31-30-2518219; E-mail: r.h.h.vandenheuvel@chem.uu.nl or robert.vandenheuvel@organon.com.

[2] The abbreviations used are: 3,5-DCP, 3,5-dichlorophenol; CHPA, 3-chloro-4-hydroxyphenylacetate; 2-Br-4-CP, 2-bromo-4-chlorophenol; CRP/FNR, cAMP receptor protein/fumarate nitrate reduction regulatory protein; 2,4-DCP, 2,4-dichlorophenol; 2,3-DCP, 2,3-dichlorophenol; HPA, 4-hydroxyphenylacetate; *m/z*, mass-to-charge; 2,4,5-TCP, 2,4,5-trichlorophenol; 2,4,6-TCP, 2,4,6-trichlorophenol; dsDNA, double-stranded DNA.

the recruitment of RNA polymerase, which then proceeds with transcription of the corresponding genes (10). Previously, a close homologue called CprK was identified in the related halorespiring bacterium, *D. dehalogenans*, which shows 91% sequence identity with CprK1 from *D. hafniense.* Upon binding of CHPA, CprK activates transcription of dehalobox-containing promoters in *D. dehalogenans* (11, 12). DNA binding studies have shown that CprK1 and CprK are only capable of binding its target DNA when the protein is in its reduced state (10, 12).

Recently, the x-ray structures of oxidized CprK1 from *D. hafniense* in complex with CHPA and reduced CprK from *D. dehalogenans* in its unliganded form have been determined by Joyce *et al.* (13). They reveal that both CprKs exhibit high structural similarity to the cAMP receptor protein (CRP) (14, 15) and PrfA, a key virulence regulator of *Listeria monocytogenes* (16). Two identical subunits form an asymmetric dimer with each monomer folded in two distinct domains: the N-terminal effector binding domain and the C-terminal DNA binding domain. The dimer interface of CprK1 is predominantly made up by the central α-helices connecting the effector binding domain with the DNA binding domain containing a helix-turn-helix motif. An intermolecular disulfide bond between Cys^{11} and Cys^{200} connects the effector binding domain to the DNA binding helix of the opposite monomer. In addition to this intermolecular disulfide bond, CrpK from *D. dehalogenans*, but not CprK1 from *D. hafniense*, has an intramolecular disulfide bond between Cys^{105}, which is conserved in FNR and most other CprK homologs and Cys^{111} (11, 12). In the x-ray structure of liganded oxidized CprK1 from *D. hafniense,* one CHPA molecule is bound per subunit in the β-barrel of the effector binding domain. The observed binding site is similar in position to the binding site of cAMP ($3',5'$-cyclic adenosine monophosphate) in CRP (13). This structure is not compatible with tight binding to dehalobox dsDNA. In the crystal structure of unliganded reduced CprK from *D. dehalogenans*, the C-terminal DNA binding domains dimerize extending to overall dimer interface, while similar DNA binding contacts are made between individual CprK dimers in the oxidized structure. Therefore, this structure is also not compatible with DNA binding.

Comparison of the two crystal structures allowed us to postulate that the binding of CHPA to CprK1 causes reorientation of the N-terminal β-barrels with respect to the central α-helix at the dimer interface and with conformational changes in the C-terminal DNA binding domains as a consequence (13). The ultimate proof of this suggestion, *i.e.* the crystal structure of effector-bound reduced CprK1 protein is not available. The present x-ray structures thus provide high resolution structural information on CprK; however, they do not provide details about protein flexibility and do not allow the continuous monitoring of *e.g.* redox- and ligand- and/or DNA-induced structural changes, which might be conformational changes and/or changes in protein dynamics.

Besides the fact that structural changes are caused by the binding of an effector molecule, it is also important to find the crucial features that enable these molecules to cause such changes. Both CprKs bind CHPA with micromolar affinity pro-

moting an interaction with dehalobox dsDNA (13). On the basis of the x-ray structures, it was suggested that: (i) the presence of the chloride group in the *ortho* position and (ii) the pK_a interrogation mechanism (formation of phenolate) allow DNA binding.

Here we report for the first time on the structural changes of CprK1 that occur during the protein activation process, *i.e.* from the oxidized unliganded form to the reduced liganded form allowing transcriptional activation. In addition, we report on the effector specificity of CprK1. For this we used a small library of potential effector molecules known to be dehalogenated by *D. dehalogenans* and *D. hafniense* in combination with macromolecular native mass spectrometry (17, 18), intrinsic fluorescence, limited proteolysis (19–21), and DNA binding assays. Native mass spectrometry was used to study oligomerization of CprK1 and interaction with potential effectors and dehalobox dsDNA, whereas limited proteolysis was used to characterize redox- and effector-induced structural changes of CprK1.

EXPERIMENTAL PROCEDURES

Preparation of CprK1 and Dehalobox dsDNA—CprK1 was overproduced and purified according to a previously established method, using *Escherichia coli* BL21 (DE3) and the pET24d-derived pWUR176 expression vector (10). CprK1 was analyzed by denaturing gel electrophoresis using a 10% (w/v) polyacrylamide gel. The gel was stained with 0.1% (v/v) Coomassie Brilliant Blue G250 for 3 min and destained overnight in 10% (v/v) acetic acid and 30% (v/v) methanol. Protein concentrations were determined using the method developed by Bradford (22). The oligonucleotide pair (5′-AGGTAAAGTTAAT-ACACATTAATACTTGCG-3′ containing an inverted repeat (dehalobox underlined) and its complementary strand) was synthesized by MWG (Ebersberg, Germany). Complementary oligonucleotides were annealed in a buffer containing 10 mM Tris, pH 7.5, 50 mM NaCl and 1 mM EDTA by heating to 95 °C and incubating at this temperature for 2 min, then cooling down slowly to room temperature. The sample buffer was exchanged to ultrapure water using Vivaspin 0.5 ml 3,000 Da cut-off columns (Vivascience, Germany).

Electrophoretic Mobility Shift Assay—A 52-bp DNA fragment from the promoter region of the *ortho*-chlorophenol reductive dehalogenase encoding *cprA1* gene was PCR-amplified from *D. hafniense* genomic DNA using oligonucleotide primers BG1748 (5′-GGTTGAGAAATTCAGGTAAAG-3′) and BG1749 (5′-GGATCACATACGCAAGTATTAATG-3′). The resulting PCR product, which contained the TTAATacacATTAA CprK1 target sequence (dehalobox), was purified and radioactively labeled at the 5′-end as described previously (10). The reaction mixtures contained POP buffer (20% (v/v) glycerol, 50 mM Tris-HCl, pH 7.5, 5 mM MgCl$_2$, 2.5 mM EDTA, 250 mM NaCl), 2.5 mM dithiothreitol, 1 μg poly(dG-dC)-poly(dG-dC), 1.5 nM ^{32}P-labeled DNA, and 0.25 μM purified CprK1 (dimer concentration). Effector compounds, if present, were added from an aqueous stock solution to a final concentration of 6.25, 20, or 200 μM. After incubation at 24 °C for 30 min, the obtained protein-DNA complexes were separated on a nondenaturing 6% (w/v) polyacrylamide gel and electrophoresed at

10 mA constant current at 4 °C in TB buffer (89 mM Tris and 89 mM boric acid). The gels were then dried, exposed to a phosphor screen for several hours, and analyzed.

Macromolecular Native Mass Spectrometry—For nanoflow electrospray mass spectrometry experiments, ultrafiltration units (ultrafree-0.5 Centrifugal Filter Device, Millipore) with a cut-off of 5,000 Da were used to exchange the buffer of CprK1 sample in 100 mM ammonium acetate, pH 8.0 (pH increased by adding ammonia). For DNA binding measurements, 5–10 mM dithiothreitol, 40–400 μM phenol derivative, 2–5 μM dehalobox dsDNA, and 4 μM Cprk1 (dimer concentration) were mixed and incubated for 30 min at room temperature. The phenols (CHPA, HPA, 2,4-DCP, 2-Br-4-CP, 2,3-DCP, 3,5-DCP, 2,4,5-TCP, and 2,4,6-TCP) were dissolved in water or in 100 mM ammonium acetate, pH 8.0. Native mass spectrometry measurements were performed in positive ion mode using an electrospray ionization time-of-flight instrument (LC-T; Micromass) equipped with a Z-spray nano-electrospray ionization source. To produce intact ions *in vacuo* from large complexes in solution, ions were cooled by increasing the pressure in the first vacuum stages of the mass spectrometer (23, 24). In addition, efficient desolvation was needed to sharpen the ion signals to determine the stoichiometry of the complexes from the mass spectrum. Therefore, source pressure conditions and electrospray voltages were optimized for transmission of the macromolecular protein complexes. The needle and sample cone voltage were 1,400 V and 140 V, respectively. The pressure in the interface region was adjusted to 8 millibars by reducing the pumping capacity of the rotary pump by closing the speedivalve. Electrospray needles were made from borosilicate glass capillaries (Kwik-Fil, World Precision Instruments) on a P-97 puller (Sutter Instruments), coated with a thin gold layer by using an Edwards Scancoat (Edwards Laboratories) six Pirani 501 sputter coater. The spectra were mass-calibrated by using a solution of 10 mg/ml cesium iodide in 50% (v/v) isopropyl alcohol.

Limited Proteolysis Coupled to Matrix-assisted Laser Desorption/Ionization Mass Spectrometry—For limited proteolysis measurements, 6 μM CprK1 (dimer concentration) was incubated in the absence or presence of 400 μM effector, 29 μM dehalobox dsDNA, and 10 mM dithiothreitol in 100 mM ammonium acetate, pH 8.0 for 30 min at room temperature. Experiments were also performed at concentrations of 600 μM for 2,4-DCP, 800 μM for 2-Br-4-CP and 2,4,6-TCP, 5 mM for 2,3-DCP, and 7 mM for 3,5-DCP. As a control, limited proteolysis was performed on the protein bovine serum albumin. These data clearly showed that the halogenated phenolic compounds do not have an effect on the proteolytic activity of trypsin. Limited proteolysis of CprK1 was performed using sequencing grade modified (0.27 μM) trypsin (Roche Applied Science). Aliquots of 2 μl of each digest were taken at 2 min, 15 min, 1 h, 6 h, and 22 h, and mixed with 8 μl of 0.2% (v/v) trifluoroacetic acid to quench trypsin activity. Trypsin digests were desalted and concentrated with μC18-ZipTips (Millipore) and analyzed on a matrix-assisted laser desorption/ionization TOF-TOF mass spectrometer (Applied Biosystems 4700 Proteomics analyzer) using α-cyano-4-hydroxycinnamic acid as the matrix. The mass spectra were recorded in positive ion reflectron mode at
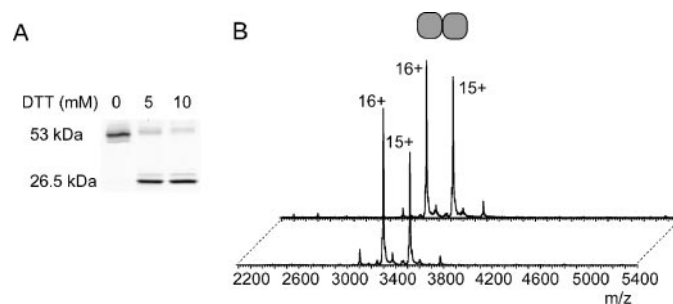

FIGURE 1. **The quaternary structure of CprK1 is independent of the protein redox state.** *A*, denaturing polyacrylamide gel of 4 μM CprK1 incubated in the presence or absence of 5 or 10 mM dithiothreitol in 100 mM ammonium acetate, pH 8. The bands observed around 26.5 and 53 kDa correspond to the reduced form (monomer) and oxidized form (dimer) of CprK1, respectively. *B*, electrospray ionization mass spectra of CprK1 sprayed from 100 mM ammonium acetate, pH 8 at a protein dimer concentration of 4 μM in the absence (*top*) or presence (*bottom*) of 10 mM dithiothreitol. Monomeric CprK1 is represented with a *square*.

20 kV accelerating voltage, and spectra were internally calibrated using the single protonated trypsin autodigestion peaks. The raw mass spectra were processed using Data Explorer software, version 4.0.

Fluorescence Measurements—Intrinsic fluorescence experiments were performed with an SPF 500c spectrofluorimeter (SLM Aminco) at 20 °C. Excitation was carried out at 280 nm, and emission fluorescence was recorded at 330 nm. A 10-mm path length quartz cell with a stirrer was used. Excitation and emission slit widths were respectively 10 and 5 nm. Halogenated phenolic compound was added to an 800-μl solution of 0.2 μM CprK1 (dimer concentration) in 100 mM ammonium acetate, pH 8.0 with 0.75 mM dithiothreitol. The observed fluorescence emission quenching was plotted against the compound concentration using KaleidaGraph (Synergy Software). The data were fitted to Equation 1,

$$F = F1 \times [L_t]/(K_d + [L_t]) \qquad \text{(Eq. 1)}$$

where *F* is the fluorescence emission at 330 nm at a given added ligand concentration, *F1* the fluorescence emission at the end of the titration, K_d the apparent dissociation constant, and $[L_t]$ the total ligand concentration (25, 26).

RESULTS

The Quaternary Structure of CprK1 Does Not Depend on the Protein Redox State—It was previously shown that oxidized CprK1 contains an intermolecular disulfide bond between Cys[11] and Cys[200] (13). We performed denaturing gel electrophoresis of CprK1 under oxidizing and reducing conditions to determine the conditions necessary to reduce CprK1 *in vitro* (Fig. 1*A*). The data clearly showed that CprK1 was almost fully reduced at pH 8 at dithiothreitol concentrations of 5 and 10 mM after incubation of 30 min at room temperature.

We studied the oligomerization state of CprK1 at pH 8 under reducing and oxidizing conditions by using native nanoflow electrospray ionization mass spectrometry (Fig. 1*B*). In both conditions, one dominant ion series was observed around 3,400 mass-to-charge (*m/z*) values corresponding to a mass of 52,739 ± 4 Da, representing dimeric CprK1. The measured mass of the dimeric species is lower than the expected mass of
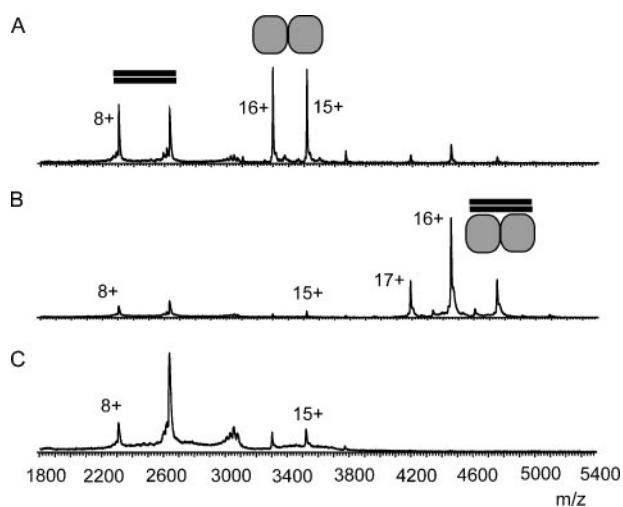
FIGURE 2. **CprK1 interacts tightly with dehalobox dsDNA under reducing conditions and in the presence of CHPA.** Electrospray ionization mass spectra of CprK1 sprayed from 100 mM ammonium acetate, pH 8 at a protein dimer concentration of 4 μM in the presence of 5 μM 30-bp dehalobox dsDNA under different conditions. *A*, in the presence of 10 mM dithiothreitol; *B*, in the presence of 10 mM dithiothreitol and 400 μM CHPA; and *C*, under oxidizing conditions and in the presence of 400 μM CHPA. Monomeric CprK1 is represented with a *square* and dsDNA with a *double line*.

the dimer (52,998 Da) on the basis of the amino acid sequence. This is caused by the deletion of the N-terminal methionine in CprK1 (expected mass 52,736 Da). In both mass spectra we also observed a low abundant species with a mass of 53,003 ± 7 Da, which is the full-length dimeric protein, thus including the N-terminal methionine. These data thus clearly indicate that the redox state of CprK1 does not influence its oligomeric state. This is in agreement with size-exclusion chromatography data from Gábor *et al.* (10), which have suggested that wild-type CprK1 and the disulfide bridge-deficient mutants [C11S]CprK1 and [C200S]CprK1 exist as a homodimer.

CprK1-mediated Dehalobox dsDNA Binding Is Induced by Reducing Conditions and the Effector CHPA—The phenol derivative CHPA is a known effector of CprK1 (10). Fig. 2*A* shows the electrospray ionization mass spectrum of CprK1 incubated with dehalobox dsDNA at pH 8 under reducing conditions. In this mass spectrum we observed three ion series around *m/z* 2,500, 3,400, and 4,400, respectively. The first series represents dehalobox dsDNA with a determined mass of 18,410 ± 3 Da (expected mass 18,407 Da). The second and third series represent dimeric CprK1 and the complex between dimeric CprK1 and one molecule of dsDNA with a determined mass of 71,165 ± 3 Da (expected mass 71,143 Da), respectively. The observed slight mass increase is likely caused by a few water or buffer molecules still present in the CprK1-dsDNA complex (27).

Fig. 2*B* shows the mass spectrum obtained after the addition of 400 μM CHPA to the dehalobox dsDNA-CprK1 solution at pH 8 under reducing conditions. The spectrum clearly shows a transition from free CprK1 and free dsDNA to a CprK1-dsDNA complex. CHPA did not induce DNA binding if the experiment at pH 8 was repeated under oxidizing conditions (Fig. 2*C*), confirming the importance of the reduction of the disulfide bridge. We did not observe interaction of CprK1 with 30-mer dsDNA having a random sequence (data not shown), strongly indicat-

ing that the interactions are specific for the DNA sequence containing the TTAAT—-ATTAA dehalobox.

Intriguingly, although the addition of CHPA enhanced efficiently the binding of DNA to CprK1, the ternary complex comprising CHPA was not observed. CHPA interacts tightly with CprK1 (0.83 μM), and the complex is also retained in the CprK1 crystals (13). Thus, in solution phase a strong interaction exists between CprK1 and CHPA, but this complex dissociates in the process of forming gas-phase ions or during the analysis of gas-phase ions in the mass spectrometer. It should be noted here that the applicability of mass spectrometry to investigate non-covalent biological complexes is strongly dependent on the nature of the interactions between the partners in the complex (28, 29). When hydrophobic interactions play a prominent role in the binding, the preservation of the complex during the electrospray measurements is highly compromised. Interactions between the acyl CoA-binding protein and ligands were not observed in conditions normally used for non-covalent complexes because hydrophobic interactions are critical to the preservation of these complexes in solution (30). Also leucine zipper complexes are poorly retained in the mass spectrometer because of the prominent role hydrophobic interactions play in these complexes (31). For CprK1, crystallographic data have shown that hydrophobic interactions play an important role in the interactions between CprK1 and CHPA. On the other hand also six hydrogen bond interactions (to Tyr[76], Gly[85], Lys[86], Thr[90], Asn[92], and Tyr[130]) and two salt bridges (with Lys[86] and Lys[133]) between the protein and CHPA are present (13). We here observe that, under the experimental conditions used, only the hydrogen bond interactions and salt bridges are not sufficient to preserve the interactions between CprK1 and its effectors in the mass spectrometer.

CprK1 Is Activated by Different Phenolic Compounds—The chlorinated phenol CHPA is a strong effector for CprK1; however, the identity of alternative effector molecules is largely unknown. We investigated the specificity of CprK1 by using a library of potential effector molecules (Fig. 3). CprK1 was mixed with dehalobox dsDNA and phenolic compound at pH 8 under reducing conditions. The effector potential of the different phenolic compounds was determined by measuring the relative amount of dsDNA-CprK1 complex formed upon incubation with the specific compound using native mass spectrometry (Fig. 4*A*). The data clearly show that both CprK1 reduction and effector binding are required for efficient dehalobox dsDNA binding. Under reducing conditions, but in the absence of a phenolic compound, a low level of complex was formed between CprK1 and the dehalobox dsDNA, which was not present under oxidizing conditions. Similarly, when reduced CprK1 was incubated with 4-hydroxyphenylacetate (HPA), a phenol derivative lacking a halogen atom at the *ortho* position, the *meta*-substituted 3,5-dichlorophenol (3,5-DCP) or cAMP, the allosteric effector for the CprK1 structural homologue CRP a low level of complex was observed, which was not present when oxidized CprK1 was incubated with these compounds. This low level of DNA binding is likely because of the reduction of the protein and not because of the presence of these compounds. The three compounds are not effectors of CprK1 (termed class I) (Fig. 3) and thus do not have an allosteric
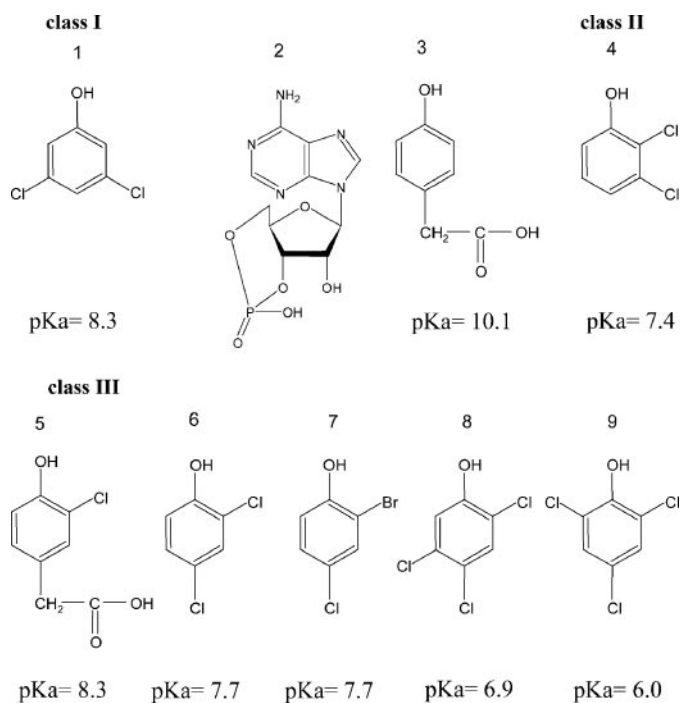
class I

1   2   3

class II

4

pKa= 8.3   pKa= 10.1   pKa= 7.4

class III

5   6   7   8   9

pKa= 8.3   pKa= 7.7   pKa= 7.7   pKa= 6.9   pKa= 6.0

FIGURE 3. **The chemical structures of the library of potential effectors for CprK1.** The molecules are classified in three classes with increasing effector activity. *class I*: 3,5-DCP (*structure 1*), cAMP (*structure 2*), and HPA (*structure 3*); *class II*: 2,3-DCP (*structure 4*); and *class III*: CHPA (*structure 5*), 2,4-DCP (*structure 6*), 2-Br-4-CP (*structure 7*), 2,4,5-TCP (*structure 8*), and 2,4,6-TCP (*structure 9*). The pK_a values are indicated.

FIGURE 4. **The effector specificity of CprK1.** *A*, diagram of electrospray ionization mass spectra of CprK1 sprayed from 100 mM ammonium acetate, pH 8 at a protein dimer concentration of 4 μM and incubated in the presence of 10 mM dithiothreitol, 5 μM 30-bp dehalobox dsDNA and 400 μM of a potential effector molecule. The diagram presents the percentage of CprK1-DNA complex formed relative to the cumulative intensity of CprK1 and CprK1-DNA complexes. *B*, electrophoretic mobility shift assays from mixtures of CprK1 and a 52-bp dehalobox dsDNA. Binding mixtures contained no protein (*lane C*) or 0.25 μM CprK1 (dimer concentration) and 6.25 μM effector molecules as indicated *above* the gel. Free dehalobox dsDNA (fast migrating band) and CprK1-DNA complexes (band with retarded electrophoretic mobility) are represented with an *open* or *filled arrow*, respectively.

effect on CprK1 by promoting protein-DNA complex formation. The compound 2,3-dichlorophenol (2,3-DCP) is a weak effector, having an allosteric effect at high concentration (400 μM) (class II), whereas CHPA, 2,4-dichlorophenol (2,4-DCP), 2-bromo-4-chlorophenol (2-Br-4-CP), 2,4,5-trichlorophenol (2,4,5-TCP), and 2,4,6-trichlorophenol (2,4,6-TCP) are already effectors at low concentration (40 μM) and thus have a strong allosteric effect on CprK1 (class III). The fact that we did not observe 100% complexation between CprK1 and DNA even in the presence of strong effectors is likely caused by incomplete reduction of the protein meaning that a low amount of oxidized protein was still present in the protein solutions (Fig. 1*A*).

The dissociation constants of the different phenol derivatives were determined by intrinsic fluorescence quenching measurements under reducing conditions (supplemental Fig. S1 and supplemental Table S1). We measured a dissociation constant of 1.4 μM for CHPA, which is in agreement with the value (0.83 μM) measured previously by Joyce *et al.* (13). All other strong effectors have dissociation constants less than 30 μM, while all other compounds have dissociation constants of more than 200 μM. Surprisingly, whereas 2,3-DCP and 3,5-DCP have similar affinities with CprK1, only 2,3-DCP is an effector for CprK1. Our data thus demonstrate the power of combining affinity assays with macromolecular mass spectrometry.

Electrophoretic mobility shift assays, using different concentrations of potential effectors (6.25, 20, and 200 μM), were performed to validate the data that were obtained by native mass spectrometry. The protein-dsDNA complexes were resolved by applying them on a non-denaturing gel. The results obtained for the interaction between dsDNA and protein in solution cor-
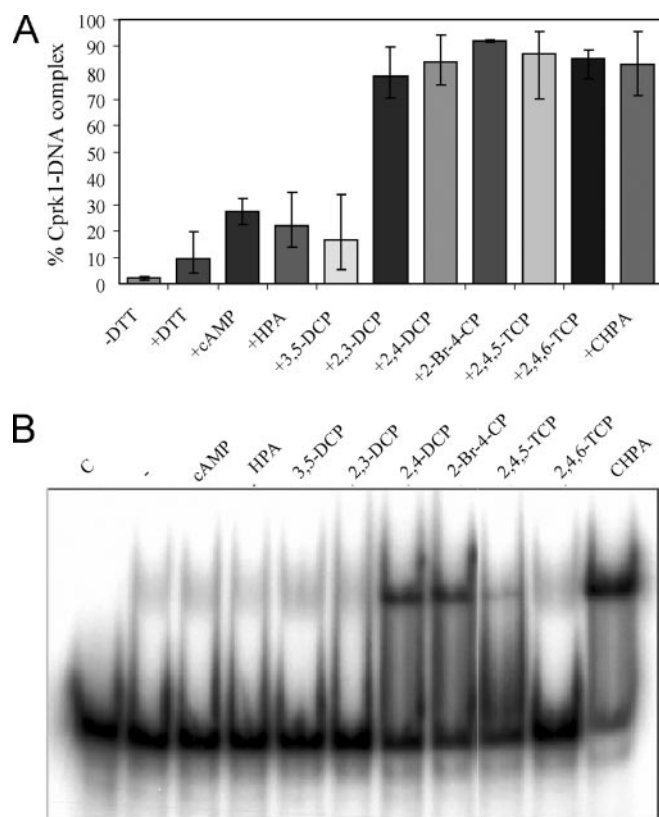
responded well with the native mass spectrometry data (Fig. 4*B*). In the absence of effector, or in the presence of HPA, 3,5-DCP, 2,3-DCP, or cAMP nearly no protein-DNA complexes were formed. The low efficiency of 2,3-DCP to form a complex is in line with the native mass spectrometry data, which showed that 2,3-DCP only forms a complex at a concentration of 400 μM and not at a concentration of 40 μM. On the other hand 2,4-DCP, 2-Br-4-CP, 2,4,5-TCP, and CHPA had an allosteric effect on CprK1 by promoting protein-dsDNA complex formation. The most prominent allosteric effect was observed for CHPA.

In contrast to the native mass spectrometry data, 2,4,6-TCP was not found to be an effector in the electrophoretic mobility shift assays, as the compound was not able, even at a concentration of 200 μM, to form protein-DNA complexes. Limited proteolysis data (see next section), however, are in line with native mass spectrometry data and showed that 2,4,6-TCP can be classified as a strong effector for CprK1, although it shows a slightly decreased protection compared with 2,4,5-TCP. The different results for 2,4,6-TCP may be explained by the different experimental set-up used. The effector role of 2,4,6-TCP may be sensitive for the buffer conditions used, which are very dif-

TABLE 1

Reaction time for the appearance of peptide bond cleavage

The reaction times for the appearance of peptide bond cleavage of oxidized CprK1, reduced CprK1, reduced CprK1 in the presence of CHPA, and reduced CprK1 in the presence of CHPA and dehalobox dsDNA are shown.

Peptide bond[a]	Identified peptides[b]	Reaction time for appearance of peptide bond cleavage			
		Oxidized CprK1	Reduced CprK1	Reduced CprK1 + CHPA	Reduced CprK1 + CHPA + DNA
Lys^8-Asp^9	T3, T4	ND[c]	15 min	ND	ND
Lys^8-Asp^9	T4-T21[d]	1 h	ND	ND	ND
$Lys^{24}-Leu^{25}$	T2, T3, T4	ND	15 min	ND	ND
$Lys^{24}-Leu^{25}$	T4-T21[d]	1 h	ND	ND	ND
$Arg^{26}-Asn^{27}$	T1	ND	2 min	ND	ND
$Arg^{26}-Asn^{27}$	T5	15 min	2 min	ND	ND
$Arg^{35}-Asp^{36}$	T6	15 min	15 min	ND	ND
$Lys^{39}-Gly^{40}$	T5	15 min	2 min	ND	ND
$Lys^{60}-Ile^{61}$	T7, T8	6 h	22 h	ND	ND
$Lys^{73}-Leu^{74}$	T9	6 h	22 h	ND	ND
$Lys^{86}-Leu^{87}$	T10	1 h	15 min	22 h	22 h
$Arg^{103}-Thr^{104}$	T10, T11	6 h	15 min	22 h	22 h
$Lys^{110}-Ser^{111}$	T11	6 h	1 h	ND	ND
$Arg^{117}-Thr^{118}$	T12, T13	6 h	22 h	ND	ND
$Lys^{128}-Asn^{129}$	T13	6 h	22 h	ND	ND
$Lys^{133}-Val^{134}$	T14	1 h	1 h	ND	ND
$Arg^{139}-Gln^{140}$	T14, T15	1 h	1 h	ND	ND
$Arg^{152}-Ile^{153}$	T15	1 h	1 h	ND	ND
$Arg^{155}-Leu^{156}$	T16, T17	22 h	15 min	15 min	15 min
$Lys^{166}-Arg^{167}$	T19	15 min	15 min	15 min	15 min
$Arg^{167}-Val^{168}$	T18	15 min	15 min	15 min	15 min
$Lys^{181}-Ser^{182}$	T20	15 min	2 min	2 min	2 min (low level)
$Arg^{196}-Val^{197}$	T20	15 min	2 min	2 min	2 min (low level)
$Arg^{196}-Val^{197}$	T21	ND	15 min	15 min	15 min
$Arg^{196}-Val^{197}$	T2-T21[d]	1 h	ND	ND	ND
$Arg^{203}-Glu^{204}$	T21	ND	15 min	15 min	15 min
$Arg^{203}-Glu^{204}$	T2-T21[d]	1 h	ND	ND	ND
$Lys^{213}-Ile^{214}$	T22	2 min	2 min	2 min	2 min
$Lys^{223}-His^{225}$	T23, T24	15 min	15 min	15 min	15 min

[a] Amino acid numbers refer to the primary amino acid sequence of CprK1.
[b] Digest fragment nomenclature refers to CprK1 protein (supplemental Fig. S2).
[c] ND, not detected at 22 hrs.
[d] Disulfide-bridged peptide.

ferent between on the one hand the DNA binding assays (POP buffer, pH 7.5) and on the other hand the mass spectrometry and limited proteolysis measurements (ammonium acetate buffer, pH 8.0). Alternatively, the 2,4,6-TCP interaction may not be compatible with the DNA binding assay.

CprK1 Dynamics Is Regulated by the Protein Redox State—The results described above show that only reduced CprK1 can be activated by an effector compound (10, 12). As the disulfide bridge between Cys^{11} and Cys^{200} is disrupted upon reduction, structural changes may be of importance for the activation process. We investigated the structural changes by using a combination of limited proteolysis and mass spectrometry, using the specific protease trypsin to partially digest CprK1. Trypsin cleaves proteins at the carboxyl side of the basic amino acids lysine and arginine, except when these two residues are followed by proline. We monitored the limited proteolysis by taking aliquots at various time points (2 min, 15 min, 1 h, 6 h, and 22 h), and analyzed the reaction mixture by matrix-assisted laser desorption/ionization mass spectrometry (supplemental Table S2 and Figs. S3, S4, S5, and S6). First, we investigated the structural changes under reducing and oxidizing conditions in the absence of effector and dehalobox dsDNA. The sequence coverage after 22 h of incubation of CprK1 was 91.3% with trypsin (Table 1 and supplemental Fig. S2). All potential trypsin cleavage sites are indicated in the model of the x-ray structure of CprK1 (Fig. 5A).

Under oxidizing conditions, the peptides T2-T21 and T4-T21 were observed after a 1-h reaction time, confirming the presence of a disulfide bridge between Cys^{11} and Cys^{200} (Table 1). These two peptides were not detected under reducing conditions. In contrast, the peptides T1, T2, T3, T4, and T21, uniquely formed when the disulfide bridge is reduced, were observed after 2 or 15 min reaction time. These non-disulfide-bridged peptides appeared at an earlier time point compared with the corresponding disulfide bridged peptides (1 h for T2-T21 and T4-T21) strongly indicating that this region of CprK1 is more dynamic under reducing conditions.

Under oxidizing conditions, 9 rapid cleavages (2 and 15 min) were observed, which are all located near the surface of the protein, and, therefore, easily accessible for trypsin (Table 1 and Fig. 5A). These potential cleavage sites were divided over the N-terminal effector binding domain (residues 1–144) and the C-terminal DNA binding domain (residues 145–232). The peptides that were formed upon cleavage at residues Arg^{26}, Arg^{35}, Lys^{39} located in the effector binding domain appeared at 15 min, those at residues Lys^{166}, Arg^{167}, Lys^{181}, Arg^{196}, and Lys^{223} located in the DNA binding domain appeared also at 15 min, but the cleavage at residue Lys^{213} corresponding to the largest C-terminal trypsin peptide appeared already at 2 min (Table 1). After 1, 6, and 22 h of incubation 6, 7, and 1 additional potential cleavage sites were observed, respectively. These peptides originate from the α-helix of the monomer-monomer interface (Arg^{117}, Lys^{128}, Lys^{133}, Arg^{139}) and from the effector binding domain including the buried β-barrels (Lys^{60}, Lys^{73}, Lys^{86}, Arg^{103}, Lys^{110}). The potential cleavage sites Lys^8, Lys^{24}, and Arg^{203} were also protected because of the disulfide bridge. Finally, the two sites
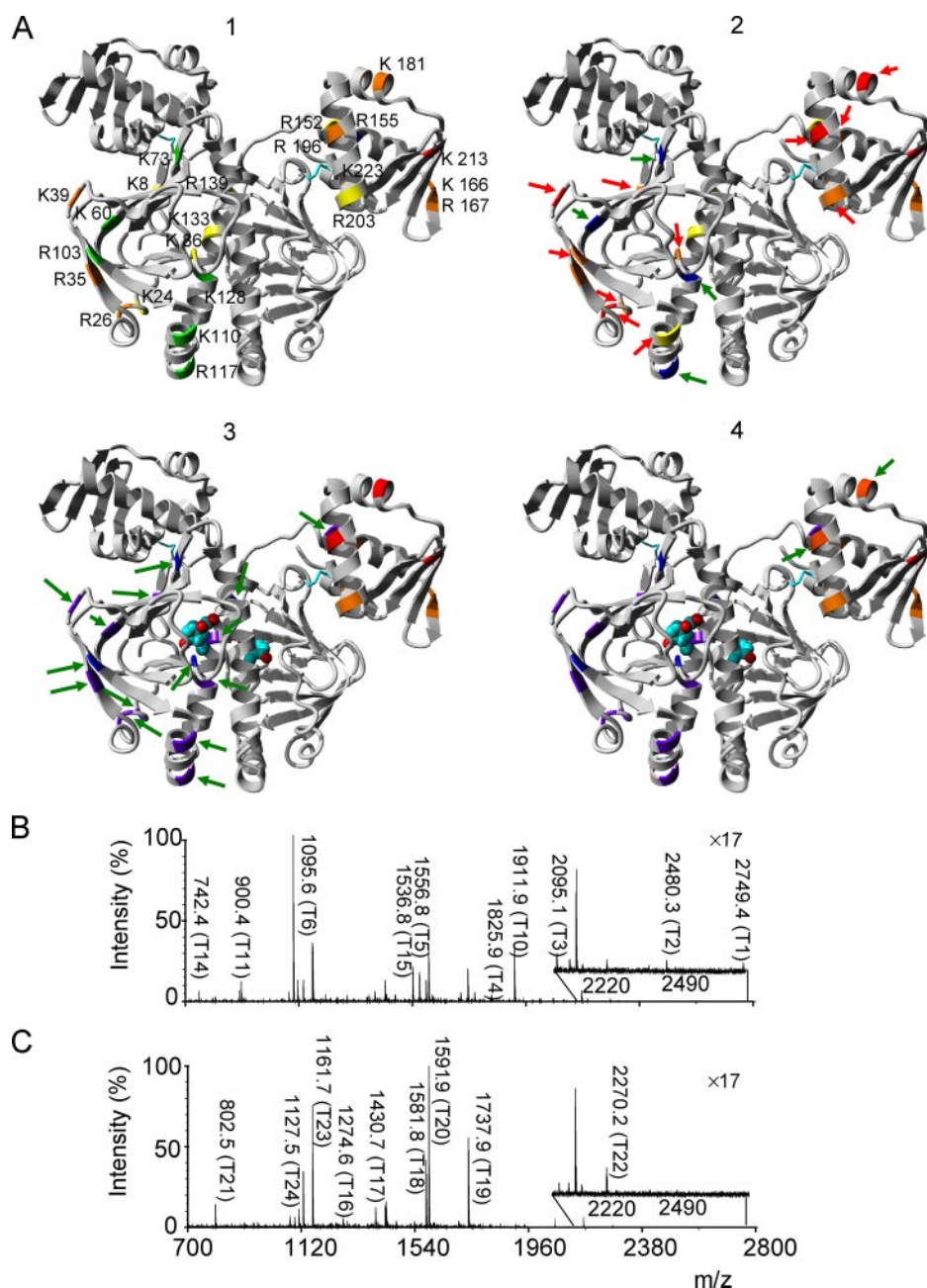
FIGURE 5. **CprK1 requires a cascade of structural changes to interact with dehalobox dsDNA.** *A*, the sensitivity of the different potential proteolytic cleavage sites are indicated in *red*, *orange*, *yellow*, *green*, *blue*, and *purple* for appearance after 2 min, 15 min, 1 h, 6 h, 22 h, and no cleavage, respectively. Low abundant peptides that appeared after 2 min are indicated in *dark orange*. For clarity, only monomer A is *color-coded*. The *arrows* show the potential cleavage sites more accessible (*red*) or more protected (*green*) under the following conditions: CprK1 under oxidizing conditions (*1*), CprK1 under reducing conditions (*2*) CprK1 under reducing conditions and in the presence of CHPA (*3*), and CprK1 under reducing conditions and in the presence of CHPA and 30-bp dehalobox dsDNA (*4*). For convenience, only the x-ray structure representing CprK1 from *D. hafniense* under oxidizing conditions and in the presence of CHPA (Protein Databank accession code 2H6B) is used. Therefore, the disulfide bond should not be present for *models 2*, *3*, and *4*. Moreover, the CHPA molecule was hidden in models 1 and 2. The figure was drawn with the free version of Yasara. *B* and *C*, matrix-assisted assisted laser desorption/ionization spectra of peptides of CprK1 after 6 h of limited proteolysis of native CprK1. CprK1 was incubated in 100 mM ammonium acetate, pH 8 at a protein dimer concentration of 6 μM, 10 mM dithiothreitol, and in the absence (*B*) or presence (*C*) of 400 μM CHPA. Trypsin was used as the proteolytic enzyme at a concentration of 0.27 μM. Peptides are labeled according to supplemental Fig. S2.

sible to trypsin compared with the oxidized form (Table 1 and Fig. 5A). The same 9 rapid potential cleavage sites were observed but 4 instead of 1 appeared already at 2 min (Arg[26], Lys[39], Lys[181], and Arg[196]). This suggests that CprK1 becomes more flexible upon reduction of the disulfide bridge, thereby facilitating trypsin cleavage. We observed 6 other rapid cleavages sites (Lys[8], Lys[24], Lys[86], Arg[103], Arg[155], and Arg[203]) at 15 min, including a site (Arg[155]) at the N-terminal part of the DNA binding domain, which was strongly protected from digestion under oxidizing conditions. Overall, the data show that under reducing conditions CprK1 becomes globally more flexible (Fig. 5A). However, 4 potential cleavage sites (Lys[60], Lys[73], Arg[117], and Lys[128]) became more protected under reducing conditions indicative for few more rigid segments or conformational changes. The reason for the protection in the effector-binding domain around Lys[60] and Lys[73] remains elusive. The residues Arg[117] and Lys[128] belong to the α-helix of the monomer-monomer interface, thus their protection may indicate a tighter interaction between the two monomers under reducing conditions.

Effector and Dehalobox dsDNA Binding Induce Structural Changes in Reduced CprK1—To study the conformational effects of effector and dehalobox dsDNA binding to CprK1, limited proteolysis experiments using trypsin were performed under reducing conditions, in the presence of the different effectors (Fig. 3) and dehalobox dsDNA. In the C-terminal DNA binding domain (residues 145–232), most cleavages were rapid (within 2 min and 15 min), irrespective of the absence or presence, type and concentration of phenol derivative used (Table 1 and Fig. 5A). The only effect in the proximity of the DNA

Arg[152] and Arg[155], which are located in the N-terminal α-helix of the DNA binding domain, showed strong protection.

Under reducing conditions, most of the potential cleavage sites located near the surface of the protein were more acces-

binding domain that resulted from the interaction with the strong effectors 2,4-DCP, 2-Br-4-CP, 2,4,5-TCP, and 2,4,6,-TCP (class III) was observed in the flexible hinge region, which connects the effector binding domain with the DNA

binding domain. In here, the cleavage site Arg[152] was fully (CHPA) or partially (other class III compounds) protected from cleavage.

In the effector binding domain (residues 1–144) 15 effector-dependent cleavages were observed. In the presence of HPA, cAMP, and 3,5-DCP, compounds that do not have an allosteric effect on CprK1 (class I and Fig. 4), and with the weak effector 2,3-DCP (class II), we did not observe any changes in the limited proteolysis pattern compared with the effector-free CprK1 pattern. For the strong effectors 2,4-DCP, 2-Br-4-CP, 2,4,5-TCP, and 2,4,6,-TCP (class III and Fig. 4), several potential cleavage sites were partially protected from proteolysis in the effector binding domain (Lys[39], Lys[86], Arg[103], Lys[110], Arg[117], Lys[128], Lys[133], and Arg[139]) in the presence of 400 μM effector. At higher concentrations, some additional potential cleavage sites were partially protected (Arg[8], Arg[24], Arg[26], Arg[35], Arg[60], Arg[73]). Incubation with the strong effector CHPA (class III) showed additional protection of most of the potential cleavage sites. Fig. 5, *B* and *C* shows the matrix-assisted laser desorption/ionization mass spectra of identified CprK1 peptides after 6 h of trypsin digestion of native CprK1 under reducing conditions in the absence or presence of CHPA. The spectra clearly show that only the peptides T16 to T24 in the C-terminal DNA binding domain are sensitive for proteolytic cleavage in the presence of CHPA. In contrast, the residues in the N-terminal effector binding domain (corresponding to peptides T1 to T15) were fully protected from cleavage in the presence of CHPA. The protected fragment T15 includes Arg[152], a residue that is positioned in the hinge region connecting the effector binding domain with the DNA binding domain.

Finally, the effect of DNA binding on the quaternary structure of CprK1 was studied by limited proteolysis mass spectrometry. When DNA binding was analyzed in the presence of the most potent effector CHPA under reducing conditions, the proteolysis pattern was very similar as compared with the proteolysis pattern of the mixture of reduced CprK1 and CHPA (Fig. 5*A*). Only the peptide T20 (residues 182–196) had a markedly decreased intensity in the presence of dsDNA after 15 min of incubation, indicating that binding of dsDNA partly protected this region from trypsin digestion. T20 covers the helix-turn-helix DNA-binding motif, which is predicted to interact with the target dsDNA (recognition α-helix, residues 191–204 in CprK1).

DISCUSSION

The transcriptional regulator CprK1 activates transcription of genes that encode proteins involved in reductive dehalogenation of chlorinated aromatic compounds (10). Despite the x-ray structures of free CprK from *D. dehalogenans* in the reduced form and the CHPA-bound CprK1 from *D. hafniense* in the oxidized form (13), the mechanism of activation, which leads to DNA binding and subsequently to transcriptional activation, is poorly understood, as these two proteins are from different sources and the active form (CHPA bound to reduced CprK) is not crystallized. However, the x-ray structures suggest that effector binding to reduced CprK induces structural rearrangement in the N-terminal β-barrels, and it has been postulated that these changes allow formation

of interdomain contacts that disrupt the DNA binding domain dimer interface leading to repositioning of the helix-turn-helix motif for DNA binding. In the present study, we monitored the activation process of CprK1 by limited proteolysis. In addition, we characterized the CprK1-effector-dehalobox dsDNA interaction and determined the effector specificity of CprK1 by multiple mass spectrometry-based methods.

Using a library of potential effector molecules, we could determine the effector specificity of CprK1. Two factors were presumed to determine the potential of a halogenated phenolic compound to act as an effector for CprK1: (i) the position and nature of the substitutions at the aromatic ring and (ii) the pK_a value for the phenol group of the molecule (13). On the basis of our data, we conclude that two substitutions at the phenolic ring are crucial for effector activity: one at the *ortho* position (chlorine or bromine) and one at the *para* position. The *ortho* chlorine atom in CHPA is positioned in van der Waals contact with the central α-helix of CprK1, which connects the effector binding domain with the DNA binding domain (13). Pop *et al.* (12) using some potential analogs of CHPA, showed a similar specificity for CprK from *D. dehalogenans*, *i.e.* the *cis*-arrangement of hydroxy and chlorine groups is optimal for activity. The substitution at the *para* position can be a halogen or an acetic acid moiety. Substitutions at position 5 and/or 6 are accepted, but not required for effector activity. Our data show that the interaction of the effector with the protein is destabilized when a chlorine is present at position 6 of the aromatic ring, because 2,4,6-TCP shows a decreased protecting effect in limited proteolysis experiments compared with 2,4,5-TCP. These data are validated by the x-ray structure of CprK1. The active site cavity clearly shows that there is some space to accommodate extra substituents at positions 3 and 5, but not at position 6 (Fig. 6).

The effector range of CprK1 (*ortho*-chlorinated phenol derivatives) shows large overlap with the substrate range of the *ortho*-chlorophenol reductive dehalogenase CprA from *D. dehalogenans* (32). The sequence of this protein is 91% identical to CprA1 of *D. hafniense* and is encoded in the same gene cluster as CprK1 (8) and activated by CprK1 on the level of transcription (10). Although *D. hafniense* DCB-2 is also capable of dechlorination of 3,5-DCP at the *meta* position (7), possibly by a yet uncharacterized reductive dehalogenase, we found that this compound was not an effector for the regulator CprK1. The partially sequenced genome of *D. hafniense* DCB-2 contains several genes that code for potential CprK-like regulators (33); therefore it is likely that either of the paralogues will have altered effector range and recognize *meta*-chlorinated phenol derivatives such as 3,5-DCP.

It was hypothesized that the high specificity of CprK1 toward CHPA is likely achieved by the "pK_a interrogation" mechanism (13). The specific recognition of CHPA would be based on the ability of CHPA to ionize to the phenolate form via deprotonation at the hydroxyl group and to consequently interact with Lys[133]. Our study clearly shows that HPA, the dechlorinated derivative of CHPA with pK_a 10.3, is not an effector for CprK1, because under physiological pH it mostly exists in its protonated form, which does not enable the molecule to make the essential salt bridge with Lys[133]. Likewise, all the phenol derivatives that have pK_a values lower than 8.3 proved to be strong
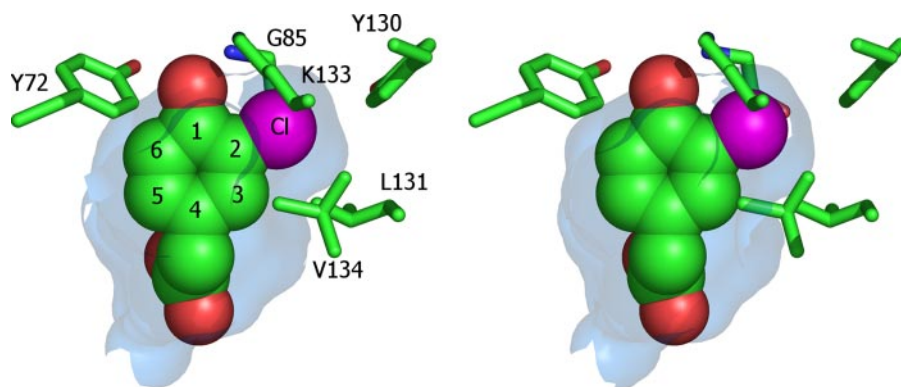
FIGURE 6. **Position of CHPA in the active site cavity of CprK1.** The stereo view drawing displays the position of CHPA within the active site cavity CprK1. The surface of the cavity is represented in *transparent blue*, CHPA with *spheres*, and key residues with *sticks*. The figure was drawn with PyMOL (W. L. DeLano (2002) The PyMOL Molecular Graphics System).
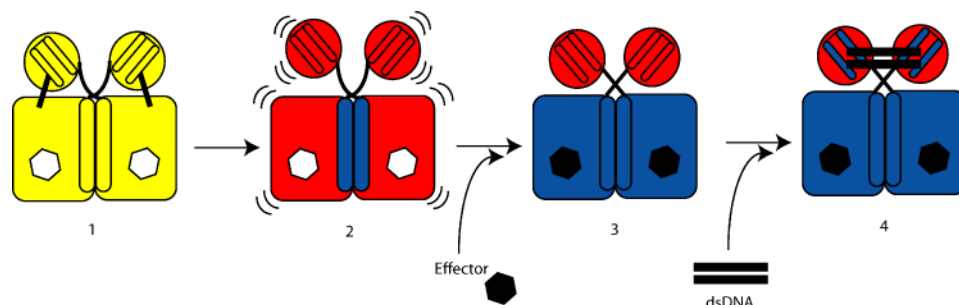

FIGURE 7. **Model describing the mechanism of activation of CprK1.** The model presents the CprK1 structural changes, which are required for dehalobox dsDNA binding. CprK1 under oxidizing conditions (*1*), CprK1 under reducing conditions (*2*), CprK1 under reducing conditions and in the presence of CHPA (*3*), and CprK1 under reducing conditions, in the presence of CHPA and 30-bp dehalobox dsDNA (*4*) (see also the legend to Fig. 5*A*). The reduction of oxidized enzyme, containing a disulfide bridge between residues Cys^{11} and Cys^{200}, results in a conformational rearrangement and increased flexibility in most regions of the protein. The α-helix forming the dimeric interface, however, shows an increased stability. The binding of an effector molecule to CprK1 induces protection and local changes in the N-terminal effector binding domain that are translated to the C-terminal DNA binding domain by changes in the hinge region (in *black*) and lead to the required conformational changes for DNA binding in the DNA binding domain and thus transcriptional activation. Finally, the binding of the dehalobox dsDNA shows protection of the peptide included in the helix-turn-helix motif. The dynamics of CprK1 dimer is indicated in *blue*, *yellow*, and *red* for low, medium, and high flexibility, respectively.

effectors for CprK1. The only exception is 3,5-DCP, which is not an effector despite its pK_a value of 8.3. Our library of potential effectors shows that both the ability to form a phenolate and the presence of a chloride group in *ortho* position are both crucial factors.

As previous *in vitro* experiments have demonstrated, CprK-like proteins are inactive under oxidizing conditions (10, 12), because of the formation of an intermolecular disulfide bridge between two monomers (13). Formation of the disulfide bridge does not change affinity of the protein to the effector CHPA compound, but affects its DNA binding capacity, probably by fixing the DNA binding domains in an inactive conformation (11, 13). It is hypothesized that such reversible inactivation of CprK-like proteins by a thiol-disulfide switch would enable the microaerophilic *Desulfitobacteria* to cope with oxidative stress (11). Interestingly, *in vivo* activity measurement in *E. coli* with a cysteine mutant of CprK1, which is unable to form the disulfide bridge, showed that the wild-type and the mutant proteins activated transcription to the same extent under aerobic growth conditions (10). This suggests that no disulfide bridge in CprK1 is formed in the cytoplasm, and as such it questions the physiological relevance of the bridge. The intriguing possibility of a

reduction step in the process of activating CprK-like transcriptional regulators was addressed in our limited proteolysis experiments. We examined three consecutive steps in the activation process of CprK1: (i) reduction of CprK1, (ii) effector binding to CprK1, and (iii) DNA binding to CprK1. The results allowed us to propose a dynamic model for the activation process of CprK1 (Fig. 7).

Oxidized CprK1 has a rigid structure because of the presence of the intermolecular disulfide bridge Cys^{11}-Cys^{200} connecting the N-terminal extremity of the first monomer with the DNA-binding helix-turn-helix motif of the second monomer. The few areas accessible to limited proteolysis in the oxidized protein are located near the surface of the protein (Fig. 5*A*). Protected areas include the dimerization α-helix and the β-barrels in the effector binding domain. Under reducing conditions the intermolecular disulfide bridge is disrupted, and the protein becomes more flexible. The cleavage frequency increased in most regions of both the N-terminal effector binding and C-terminal DNA binding domain. The x-ray structure of the reduced form of CprK from *D. dehalogenans* reveals that, in contrast with the

oxidized form of CprK1 from *D. hafniense* the DNA binding domains of two monomers form multiple interactions with each other (residues 152–164 and 180–187) (13). Our limited proteolysis results, however, show that residues Arg^{155} and Lys^{181} are not protected upon reduction, strongly indicating that these interactions are not stable in solution. Intriguingly, the dimerization α-helix becomes more protected when the disulfide bonds are reduced, indicating that packing interactions in the monomer-monomer interface become stronger upon reduction. Joyce *et al.* (13) have demonstrated that the positions of the dimerization α-helix were the same in both the reduced and the oxidized structure. We speculate that the tighter monomer-monomer interactions allow the protein to be more flexible in other regions without losing its stability.

Although the reduction of the protein is a prerequisite for DNA binding, our results clearly show that it has to be accompanied by the binding of an effector molecule to enable CprK1 to form a complex with dehalobox dsDNA. Effector binding induces structural changes in the effector binding domain of CprK1, shown by the protection of potential cleavage sites in this domain upon effector molecule binding. Protection was most effective with the strong effector molecules 2,4-DCP,

2-Br-4-CP, 2,4,5-TCP, and 2,4,6-TCP. This is in agreement with the x-ray structure, which shows that binding of CHPA reduces the volume of the hydrophobic pocket (shift in the position of Gly[85], reorientation of Tyr[130] and Leu[131]) and stabilizes the structure by more interactions (Lys[86] interacts with the acetic group, which is also hydrogen bound to Thr[90] and Asn[92]) (13). In addition, we observed a strong stabilization effect in the interface α-helix. In contrast, the C-terminal DNA binding domain proved to be sensitive to protease digestion, irrespective of the absence or presence of effectors. However, an important exception was Arg[152], a residue situated in the hinge region, which connects the effector binding domain with the DNA binding domain. In the presence of CHPA it was fully protected from cleavage. This indicates that this region may be involved in transmitting the effector binding signal from the effector binding domain to the DNA binding domain allowing the correct positioning of the helix-turn-helix motif for DNA binding. Indeed, mutations in the corresponding hinge region of *E. coli* CRP (A144T) and *Listeria monocytogenes* PrfA (G145S) resulted in a constitutively active DNA binding conformation of these proteins, giving further support to our hypothesis (16, 34).

Finally, we showed that DNA binding protected a 14-amino acid peptide (T20) from trypsin digestion. This peptide is part of the recognition α-helix in the helix-turn-helix DNA binding motif of CprK1 and contains the V-SR conserved motif, which is known to be involved in contacting the specific TTAAT—-ATTAA dehalobox DNA sequence (10). The results of the limited proteolysis experiments thus provide evidence that CprK1 makes a contact with its specific dsDNA target via the second helix of the helix-turn-helix motif, similar to other members of the CRP-FNR family of proteins (35).

In conclusion, the results presented reveal the effector specificity of CprK1 and provide insight in the structural changes involved in the activation process of CprK1. The data extend the knowledge on the molecular basis of transcriptional activation of halorespiration.

REFERENCES

1. Smidt, H., and de Vos, W. M. (2004) *Annu. Rev. Microbiol.* **58,** 43–73
2. El Fantroussi, S., Naveau, H., and Agathos, S. N. (1998) *Biotechnol. Prog.* **14,** 167–188
3. Holliger, C., Wohlfarth, G., and Diekert, G. (1999) *FEMS Microbiol. Rev.* **22,** 383–398
4. Utkin, I., Woese, C., and Wiegel, J. (1994) *Int. J. Syst. Bacteriol.* **44,** 612–619
5. Utkin, I., Dalton, D. D., and Wiegel, J. (1995) *Appl. Environ. Microbiol.* **61,** 346–351
6. Christiansen, N., and Ahring, B. K. (1996) *Int. J. Syst. Bacteriol.* **46,** 442–448
7. Madsen, T., and Licht, D. (1992) *Appl. Environ. Microbiol.* **58,** 2874–2878
8. Christiansen, N., Ahring, B. K., Wohlfarth, G., and Diekert, G. (1998) *FEBS Lett.* **436,** 159–162
9. Smidt, H., van Leest, M., van der Oost, J., and de Vos, W. M. (2000) *J. Bacteriol.* **182,** 5683–5691
10. Gábor, K., Veríssimo, C. S., Cyran, B. C., Ter Horst, P., Meijer, N. P., Smidt, H., de Vos, W. M., and van der Oost, J. (2006) *J. Bacteriol.* **188,** 2604–2613
11. Pop, S. M., Gupta, N., Raza, A. S., and Ragsdale, S. W. (2006) *J. Biol. Chem.* **281,** 26382–26390
12. Pop, S. M., Kolarik, R. J., and Ragsdale, S. W. (2004) *J. Biol. Chem.* **279,** 49910–49918
13. Joyce, M. G., Levy, C., Gábor, K., Pop, S. M., Biehl, B. D., Doukov, T. I., Ryter, J. M., Mazon, H., Smidt, H., van den Heuvel, R. H., Ragsdale, S. W., van der Oost, J., and Leys, D. (2006) *J. Biol. Chem.* **281,** 28318–28325
14. Harman, J. G. (2001) *Biochim. Biophys. Acta* **1547,** 1–17
15. Fic, E., Polit, A., and Wasylewski, Z. (2006) *Biochemistry* **45,** 373–380
16. Eiting, M., Hageluken, G., Schubert, W. D., and Heinz, D. W. (2005) *Mol. Microbiol.* **56,** 433–446
17. van den Heuvel, R. H., and Heck, A. J. (2004) *Curr. Opin. Chem. Biol.* **8,** 519–526
18. Hanson, C. L., and Robinson, C. V. (2004) *J. Biol. Chem.* **279,** 24907–24910
19. Akashi, S. (2006) *Med. Res. Rev.* **26,** 339–368
20. McDonald, C., and Li, L. (2005) *Anal. Chim. Acta* **534,** 3–10
21. Myers, S. L., Thomson, N. H., Radford, S. E., and Ashcroft, A. E. (2006) *Rapid Commun. Mass Spectrom.* **20,** 1628–1636
22. Bradford, M. M. (1976) *Anal. Biochem.* **72,** 248–254
23. Tahallah, N., Pinkse, M., Maier, C. S., and Heck, A. J. (2001) *Rapid Commun. Mass Spectrom.* **15,** 596–601
24. Krutchinsky, A. N., Chernushevich, I. V., Spicer, V. L., Ens, W., and Standing, K. G. (1998) *J. Am. Soc. Mass Spectrom.* **9,** 569–579
25. Clarke, A. (1996) *Enzymology LabFax*, pp. 199–221, Academic Press, San Diego
26. Brandes, H. K., Larimer, F. W., Lu, T. Y., Dey, J., and Hartman, F. C. (1998) *Arch. Biochem. Biophys.* **352,** 130–136
27. Sobott, F., McCammon, M. G., Hernandez, H., and Robinson, C. V. (2005) *Philos. Transact. A. Math. Phys. Eng. Sci.* **363,** 379–391
28. Rogniaux, H., Sanglier, S., Strupat, K., Azza, S., Roitel, O., Ball, V., Tritsch, D., Branlant, G., and Van Dorsselaer, A. (2001) *Anal. Biochem.* **291,** 48–61
29. Loo, J. A. (1997) *Mass Spectrom. Rev.* **16,** 1–23
30. Robinson, C. V., Chung, E. W., Kragelund, B. B., Knudsen, J., Aplin, R. T., Poulsen, F. M., and Dobson, C. M. (1996) *J. Am. Chem. Soc.* **118,** 8646–8653
31. Wendt, H., Durr, E., Thomas, R. M., Przybylski, M., and Bosshard, H. R. (1995) *Protein Sci.* **4,** 1563–1570
32. van de Pas, B. A., Smidt, H., Hagen, W. R., van der Oost, J., Schraa, G., Stams, A. J., and de Vos, W. M. (1999) *J. Biol. Chem.* **274,** 20287–20292
33. Villemur, R., Saucier, M., Gauthier, A., and Beaudet, R. (2002) *Can. J. Microbiol.* **48,** 697–706
34. Weber, I. T., Gilliland, G. L., Harman, J. G., and Peterkofsky, A. (1987) *J. Biol. Chem.* **262,** 5630–5636
35. Green, J., Scott, C., and Guest, J. R. (2001) *Adv. Microb. Physiol.* **44,** 1–34